J Supercond Nov Magn (2010) 23: 1289–1294
DOI 10.1007/s10948-010-0771-3

ORIGINAL PAPER

Effects of Out-of-Plane Disorder in $CaFe_{1-x}Co_xAsF$ System

Changjin Zhang · Min Zhang · Shun Tan · Chuanying Xi · Lei Zhang · Langsheng Ling · Wei Tong · Yuheng Zhang

Received: 25 February 2010 / Accepted: 19 March 2010 / Published online: 7 April 2010

Abstract We perform oxygen doping experiments in the CaFeAsF and $CaFe_{0.88}Co_{0.12}AsF$ compounds. In the parent compound CaFeAsF, partial replacement of F by O leads to an increase of resistivity and a weakening of spin-density wave transition, indicating that the out-of-plane disorder strongly affects the electronic and magnetic properties of the system. In the $CaFe_{0.88}Co_{0.12}AsF_{1-x}O_x$ system, the doping of oxygen leads to the suppression of superconductivity, reflecting the importance of Ca–F layer disorder in this system.

Keywords CaFeAsF · Spin-density wave transition · Electron spin resonance

1 Introduction

The recent discovery of superconductivity at T_c's up to 56 K in iron pnictide systems [1–4] has sparked enormous interest in this class of materials. The ground state of iron pnictide systems has been revealed to be bad metal. With the doping of charge carriers, the ground state of FeAs compounds evolves from a spin-density-wave (SDW) state to a superconducting state [5]. In the *RE*FeAsO (*RE*, rare earth elements) systems, superconductivity can be achieved by either Fe-site doping or O-site doping, i.e., partial substitution of Fe by Co (Ni) or substitution of O by F. Besides the *RE*FeAsO-based superconductors, it is interesting to discover another CrCuSiAs-type superconductors, i.e., CaFeAsF-based superconductors, which contain no oxygen atoms [6]. The parent compounds, *RE*FeAsO and CaFeAsF, are both bad metals exhibiting spin-density wave transition below 150 K. Superconductivity emerges upon charge carrier doping, while SDW transition is suppressed in the superconducting regime [7, 8].

Both the *RE*FeAsO system and the CaFeAsF system have a layered structure, where the conducting Fe_2As_2 layers are isolated from the charge reservoir layers so that the doped carriers (holes or electrons) can move within the conducting layers. In both systems, superconductivity can be achieved by partial substitution of Fe by Co or Ni. Since the superconductivity in the *RE*FeAsO systems can be achieved by partial substitution of O by F, it is interesting to explore whether or not the superconductivity in the CaFeAsF system can be induced by partial substitution of F by O. In this work we perform oxygen-doping experiments on both the parent compound CaFeAsF and the Co-doped superconductor $CaFe_{0.88}Co_{0.12}AsF$. The lattice structure, transport and magnetic properties, as well as the optical response of the O-doped systems are explored.

2 Experimental Detail

The polycrystalline samples with nominal composition $CaFeAsF_{1-x}O_x$ and $CaFe_{0.88}Co_{0.12}AsF_{1-x}O_x$ ($x = 0, 0.05, 0.1, 0.2$) were prepared by conventional solid-state reaction method using high-purity Ca_3As_2, Fe_3As_2, Co_3As_2, CaF_2 (powder, 99.999%, Alfa-Aesar) and CaO (powder,

C. Zhang (✉) · C. Xi · L. Zhang · L. Ling · W. Tong · Y. Zhang
High Magnetic Field Laboratory, Chinese Academy of Sciences, Hefei 230031, People's Republic of China
e-mail: zhangcj@hmfl.ac.cn

M. Zhang · S. Tan · Y. Zhang
Hefei National Laboratory for Physical Sciences at Microscale, University of Science and Technology of China, Hefei 230026, People's Republic of China

99.95%, Alfa-Aesar) as starting materials. Ca_3As_2 was synthesized by heating Ca (granules, redistilled, 99.5%, Alfa-Aesar) with As (powder, 99.99%, metal basis, Alfa-Aesar) at 600 °C for 10 hours in an evacuated silica tube. Fe_3As_2 and Co_3As_2 were prepared from powders of mixed elements at 750 °C for 6 hours. The raw materials were thoroughly ground and pressed into pellets. The pellets were wrapped up by Ta foil and sealed in an evacuated quartz tube. They were preheated at 1000 °C for 10 hours and cooled down slowly to room temperature. The pellets were ground again and pressed into pellets and heated at 1000 °C for 12 hours.

X-ray diffraction (XRD) was carried out by a Rigaku-D/max-gA diffractometer using high-intensity Cu$K\alpha$ radiation to screen for the presence of an impurity phase and the changes in structure. The lattice parameters were determined from the d-value of XRD peaks by a standard least-squares refinement method. The measurements of infrared (IR) transmission spectra (Nicolet 700) were carried out at room temperature with powder samples in which KBr was used as a carrier. The resistivity was measured using a standard four-probe method in a closed-cycle helium cryostat. The magnetic susceptibility of the samples was determined by a SQUID magnetometer (Quantum Design, MPMS). The applied magnetic field was 10 Oe with both zero-field-cooling and field-cooling. The electron paramagnetic resonance (EPR) measurements were performed at 9.46 GHz using a Bruker ER-200D spectrometer.

3 Results and Discussion

Figure 1 shows the X-ray diffraction patterns of the $CaFeAsF_{1-x}O_x$ and $CaFe_{0.88}Co_{0.12}AsF_{1-x}O_x$ samples. The powder XRD results reveal the formation of nearly single-phase products for samples with $0 \leq x \leq 0.2$. The minor impurity peaks, which reflect very small amount of un-reacted impurities, such as CaF_2 and Fe_2As, are marked in Fig. 1. The index of diffraction peaks has been marked to be tetragonal [9]. It is apparent that there is no macroscopic structure phase transition with increasing O-doping content. In order to investigate in detail the effect of O doping in the crystal lattice, we calculate the lattice parameters of the samples. The calculated values of the a and c axes are listed in Table 1. In both systems, it is found that the doping of O hardly affects the a-axis lattice parameter, while the c-axis lattice parameter exhibits an apparent expansion with increasing O doping. The expansion of c-axis lattice parameter seems to be linked with the larger ion radius of O comparing to that of F.

In order to explore further the doping effects of O^{2-}, the phonon vibration modes of the samples have been investigated by means of infrared absorption measurements, because the optical vibration modes are effective to reflect the change of lattice parameters and conductive properties. Early theoretical calculations of the optical phonon modes of the LaFeAsO system have revealed that the optical phonon dispersions can be divided into two regions [10]. Below $\sim$300 cm^{-1} the dispersions are dominated by metal and As modes of mixed character, while the modes above $\sim$300 cm^{-1} are strongly O-derived. In the

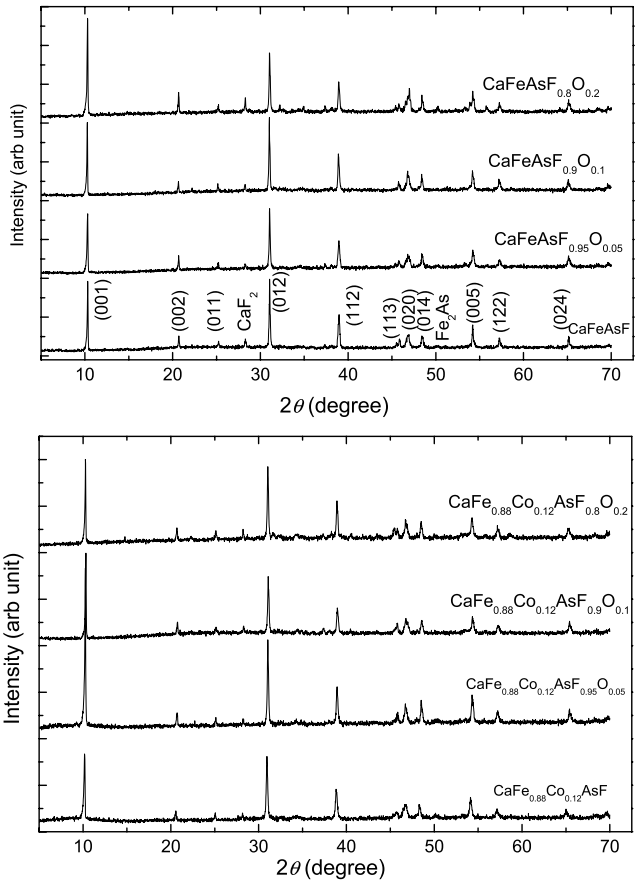

Fig. 1 Powder X-ray-diffraction patterns of polycrystalline samples $CaFeAsF_{1-x}O_x$ and $CaFe_{0.88}Co_{0.12}AsF_{1-x}O_x$

Table 1 The unit cell parameters of the $CaFeAsF_{1-x}O_x$ and $CaFe_{0.88}Co_{0.12}AsF_{1-x}O_x$ samples

$CaFeAsF_{1-x}O_x$	a (Å)	c (Å)	$CaFe_{0.88}Co_{0.12}AsF_{1-x}O_x$	a (Å)	c (Å)
$x = 0$	3.89502	8.50062	$x = 0$	3.8898	8.46351
$x = 0.05$	3.89526	8.50602	$x = 0.05$	3.88926	8.47354
$x = 0.1$	3.89506	8.51185	$x = 0.1$	3.88998	8.48062
$x = 0.2$	3.89512	8.53233	$x = 0.2$	3.88981	8.48833

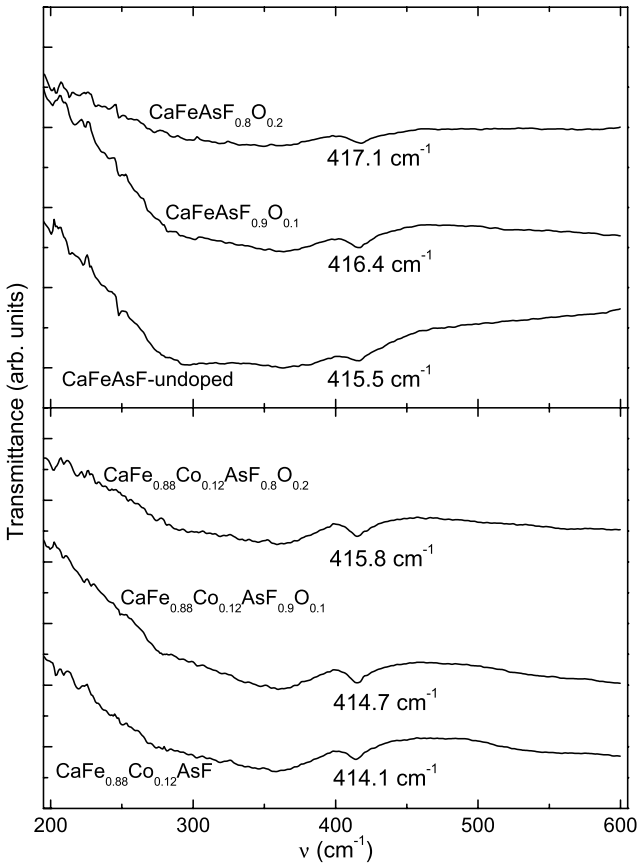

Fig. 2 The infrared transmission spectra of the $CaFeAsF_{1-x}O_x$ and $CaFe_{0.88}Co_{0.12}AsF_{1-x}O_x$ samples

CaFeAsF system, we consider that the F-derived phonon modes also lie above 300 cm^{-1}, and the doping of oxygen mainly affects these phonon modes. Figure 2 shows the mid-infrared absorption spectra of the $CaFeAsF_{1-x}O_x$ and $CaFe_{0.88}Co_{0.12}AsF_{1-x}O_x$ samples. We find a predominate peak locating at about 415 cm^{-1}. We compare the mid-infrared spectra of the CaFeAsF system with that of the *RE*FeAsO systems. In the *RE*FeAsO systems, the E_g oxygen mode is predicted to be at 434 cm^{-1} for $RE = La$ [11], at 503 cm^{-1} for $RE = Sm$ [12], at 450 cm^{-1} for $RE = Ce$ [13], and at 485 cm^{-1} for $RE = Nd$ [14]. Compared to these results, the absorption peak observed at around 415 cm^{-1} in $CaFe_{1-x}Co_xAsF$ system is assigned to the E_g fluorine mode, which involves the optical phonon along the *c*-axis.

With increasing O doping, the infrared absorption peak at around 415 cm^{-1} slightly shifts to higher frequency in both the $CaFeAsF_{1-x}O_x$ and the $CaFe_{0.88}Co_{0.12}AsF_{1-x}O_x$ systems. We consider that the locations of infrared active modes in a crystal are determined by two factors: the bond strength (or bond length) of the mode involved and the ionic masses. In the present case, there is a competition between these two factors. Since the lattice parameter along *c*-axis expands with increasing O-doping content, the infrared peak would shift to lower frequency. However, as the ionic mass of O is lighter than that of F, the phonon peak should thus shift to higher frequency. In the $CaFeAsF_{1-x}O_x$ and the $CaFe_{0.88}Co_{0.12}AsF_{1-x}O_x$ systems, the competition of the two factors results in a net shift toward higher frequency. The gradual shift of the E_g mode with increasing oxygen doping confirms that part of the fluorine site is substantially replaced by oxygen.

The transport and magnetic properties of the $CaFe_{1-x}Co_xAsF$ superconducting compounds have previously been studied by several groups [6, 15, 16]. The present results on these samples in general agree with previous reports. For example, the temperature dependence of resistivity and magnetic susceptibility of the $CaFe_{1-x}Co_xAsF$ ($x = 0, 0.12$) are shown in Figs. 3 and 4, respectively. For the undoped CaFeAsF, the magnetic susceptibility exhibits a decrease with decreasing temperature at high temperature, indicating a non-paramagnetic character. In order to learn the magnetic state at this stage, we perform the magnetic field dependence of magnetization (M–H curve) measurement at 300 K, the result of which is shown in the inset of Fig. 4(a). It is clear that there is a coexistence of ferromagnetic and paramagnetic signals at 300 K. This fact indeed indicates that superconductivity occurs in a parent compound of ferromagnetic background. With decreasing temperature, the magnetic order in the form of SDW sets in at about 110 K in the parent compound CaFeAsF. The SDW transition leads to a decrease in magnetic susceptibility and a sharp decrease in resistivity. In the optimally doped $CaFe_{0.88}Co_{0.12}AsF$, the SDW order is completely suppressed. Interestingly, we find that in the $CaFe_{0.88}Co_{0.12}AsF$ sample, there exhibits a metal-insulating transition at around 120 K, where a weak increase of magnetic susceptibility occurs. So far no one has explained this Co-induced metal-insulating transition in this system.

In order to learn the magnetic states of the $CaFe_{1-x}Co_xAsF$ samples in detail, we perform electron spin resonance (ESR) measurements on these samples between 1.9 K and 300 K, the results of which are shown in Fig. 5. The benefit of ESR is that it can give us dynamic magnetic information about the local moment. At 300 K, we notice that there is a weak paramagnetic signal locating at about 3380 Oe in CaFeAsF sample (see Fig. 5(a)). Besides the paramagnetic signal, one can clearly see that there is a broad peak which is below the paramagnetic resonance field (∼3380 Oe in present instrument). Compared with the M–H curve in Fig. 4(a), this broad peak seems to be originated from the ferromagnetic signal. It is found that this peak almost disappears at low temperature, which is consistent with the occurrence of the SDW transition. This fact gives us solid evidence that the ferromagnetic signal presented in the CaFeAsF system is not originated from magnetic impurities. That is, the existence of ferromagnetic signal is an intrinsic behavior. For the $CaFe_{0.88}Co_{0.12}AsF_{1-x}O_x$ sample, the ESR spectra shown in Fig. 5(b) exhibit complicated

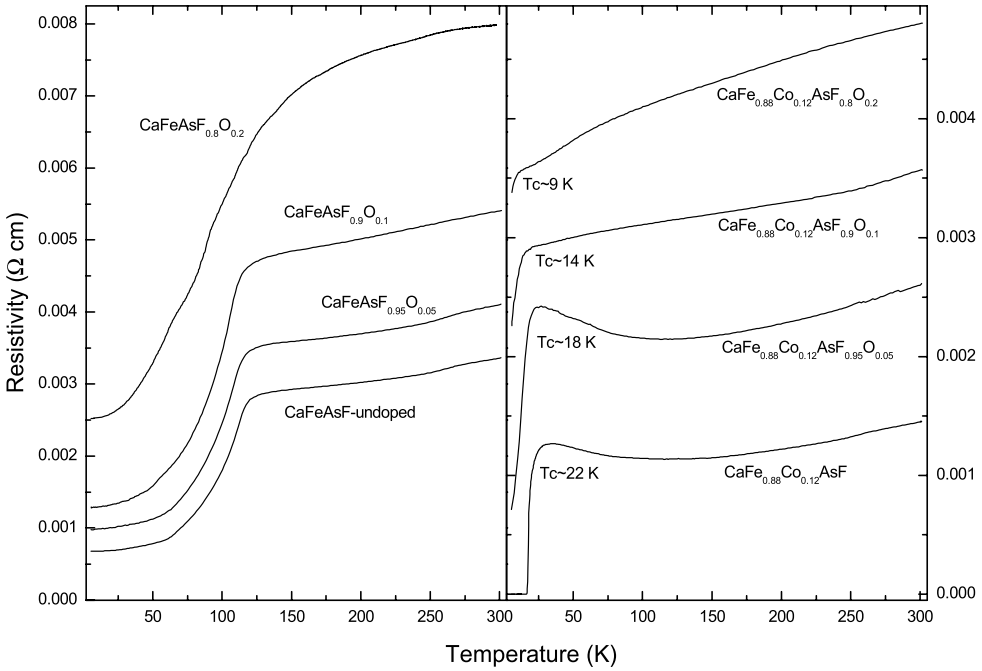

Fig. 3 The temperature dependence of resistivity of the $CaFeAsF_{1-x}O_x$ and $CaFe_{0.88}Co_{0.12}AsF_{1-x}O_x$ samples

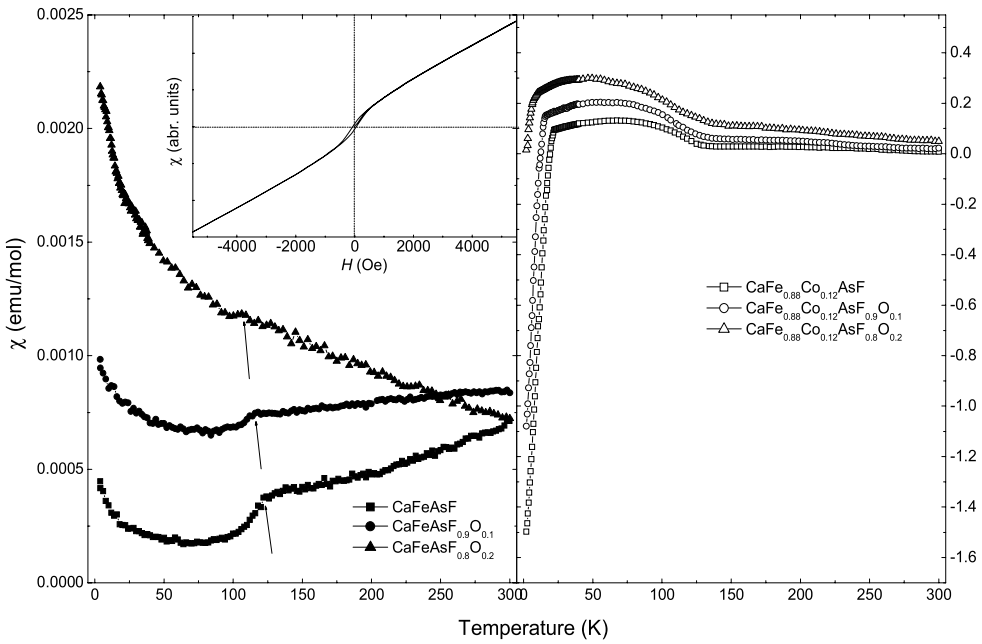

Fig. 4 The temperature dependence of magnetic susceptibility of the $CaFeAsF_{1-x}O_x$ and $CaFe_{0.88}Co_{0.12}AsF_{1-x}O_x$ samples. The *inset* in (**a**) shows the $M-H$ curve for undoped CaFeAsF at 300 K. In order to see it clearly, only the data below $H = 6000$ Oe is given

behaviors. The ESR spectrum taken at 300 K is shown in the inset, which is quite similar to that of CaFeAsF parent compound. With decreasing temperature, the paramagnetic signal strengthens. The resonance signal exhibits very complicated hyperfine structure below ∼120 K, which is consistent with the metal-insulating transition (and the weak increase of magnetic susceptibility) in this sample. This fact gives us another important clue that the increase of magnetic susceptibility at about 120 K is not originated from a small amount of ferromagnetic impurity such as FeAs:Co as previously supposed [6]. This complicated hyperfine structure indicates magnetic inhomogeneities and phase separations in Co-doped samples. This result also supports the insular superconductivity concluded from muon spin rotation measurements [17]. Cobalt doping in this system induces strong randomness across the phase boundaries. The overlap between different regimes would be very important in determining the transport and magnetic behaviors in this system. It is reasonable to conclude that the electron hopping interaction constant (via the overlap) between the Fe $3d$ electrons and the As $3p$ electrons is different from the hopping constant between the Co $3d$ electrons and As electrons. Thus

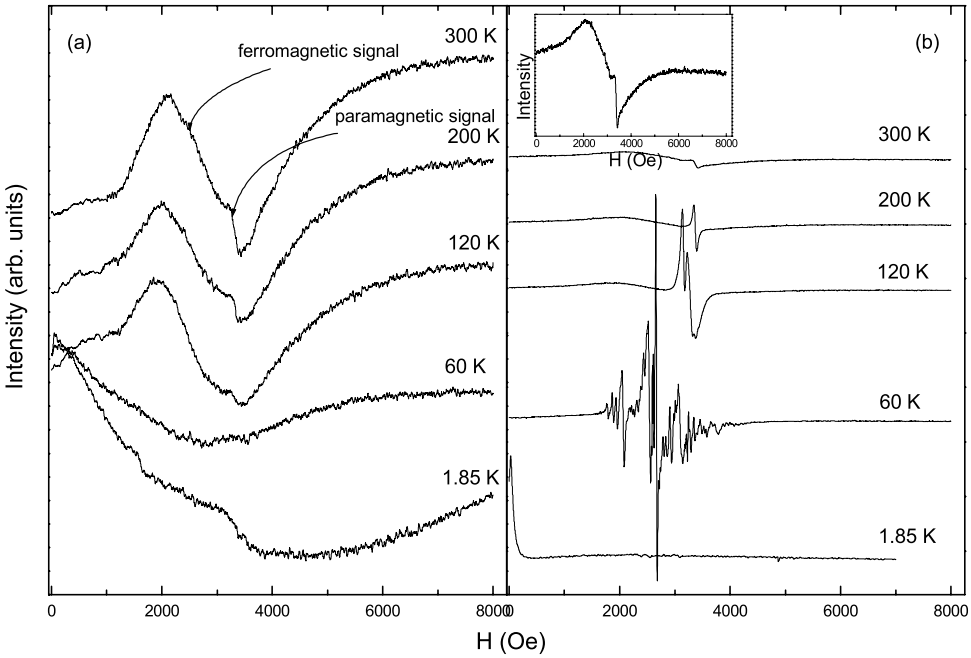

Fig. 5 Electron spin resonance spectra at different temperatures for (**a**) CaFeAsF and (**b**) $CaFe_{0.88}Co_{0.12}AsF$. The *inset* of (**b**) shows an enlarged view for the 300 K data

the energy gap for the Fe–As regions is different from that for the Co–As regions. This difference would induce a net energy gap in the $CaFe_{1-x}Co_xAsF$ system, which might be the reason for the Co-induced metal-insulating transition at around 120 K.

Figures 3 and 4 give the temperature dependences of resistivity and magnetic susceptibility of the $CaFeAsF_{1-x}O_x$ and $CaFe_{0.88}Co_{0.12}AsF_{1-x}O_x$ samples. The temperature dependence of resistivity of the parent compound CaFeAsF exhibits poor metallic behavior at high temperature, followed by a sharp decrease at 110 K, which is linked to the SDW anomaly [7, 8]. In the $CaFeAsF_{1-x}O_x$ samples, it is interesting to find that the SDW anomaly appears in the resistivity curves for all samples. The SDW transitions are also indicated in the χ–T curves for all samples. This is in sharp contrast to that in REFeAsO$_{1-x}$F$_x$, where the SDW transition is severely suppressed with several percent of F doping [1–4]. In the REFeAsO$_{1-x}$F$_x$ system, it is believed that the REO(F) layers are the charge reservoir layers. With the substitution of O by F, electron-type charge carriers are introduced into the compound. The charge carriers are eventually transferred from the charge reservoir layers into the FeAs conduction layers due to the coupling between these layers. The SDW transition is depressed due to the strong mobility of the charge carriers. In the $CaFeAsF_{1-x}O_x$ system, it is natural to believe that the substitution of F by O in $CaFeAsF_{1-x}O_x$ would introduce hole-type charge carriers. However, it is quite strange that the introduced hole carriers do not lead to the suppression of SDW transition. We conclude that the only way to explain this behavior is to assume that the carriers induced by O doping are not transferred into the Fe_2As_2 layers in the $CaFeAsF_{1-x}O_x$ system. This conclusion is supported by the increased resistivity with increasing O-doping concentration.

It is interesting to explore further why the introduced hole carriers are not transferred into the Fe_2As_2 conduction layers in the $CaFeAsF_{1-x}O_x$ system. In order to clarify this puzzle, we check the c-axis lattice parameters of the $CaFe_{1-x}Co_xAsF$ superconductors where the electron carriers are introduced into the Fe_2As_2 conduction layers. The c-axis lattice parameter shortens monotonously with increasing Co-doping concentration [18]. We also check the c-axis lattice parameters of some other iron pnictide superconductors such as REFeAsO$_{1-x}$F$_x$ [19, 20], REFe$_{1-x}$Co$_x$AsO [21], BaFe$_{2-x}$Ni$_x$As$_2$ [22], etc. It is found that in these superconducting systems, the introduction of charge carriers into the Fe–As conduction layers all results in a shortening of the c-axis lattice parameter. Thus it seems that the transfer of charge carriers from the charge reservoir layer into the Fe–As conduction layer generally leads to a shortened c-axis parameter. In order words, a shortened c-axis lattice distance favors the charge transfer. In the $CaFeAsF_{1-x}O_x$ system, the calculated c-axis lattice parameter slightly increases with increasing O-doping content, which is unfavorable to the charge transfer.

In the $CaFe_{0.88}Co_{0.12}AsF_{1-x}O_x$ system, the substitution of F by O leads to an increase of resistivity, similar to that in the $CaFeAsF_{1-x}O_x$ system. We also notice that partial substitution of F by O leads to the suppression of superconductivity. The superconducting transition temperature, T_c, deceases monotonously with increasing O content. According to the conclusion taken from the $CaFeAsF_{1-x}O_x$ case, the O doping does not lead to any charge transfer from the

Ca–F(O) layer to the Fe–As layer. The suppression of superconductivity seems not to originate from the decrease of charge carrier concentration. As O^{2-} ions are not magnetic ions, the suppression of superconductivity does not come from the well-known magnetic pair-breaking effects [23]. We consider the O doping introduces out-of-plane disorder in the system. This type of disorder works as weak scatterers in contrast to the strong randomness induced by in-plane Co doping [17], but remarkably reduces T_c, suggesting novel effects of disorder on the superconductivity. The effects of out-of-plane disorder on T_c in oxypnictide superconductor $RE\mathrm{FeAsO}_{1-x}\mathrm{F}_x$ (RE = Nd, Ce–Gd, and La–Dy) have also been suggested by using extended X-ray absorption fine structure measurements [24]. We also notice that in cuprate superconducting systems such as $\mathrm{Bi_2Sr_2CuO_6}$ and $\mathrm{La_{2-x}Sr_xCuO_4}$, similar effects of out-of-plane disorder on T_c have been revealed [25]. All these experimental results suggest that the out-of-plane disorder works as weak scatterers, but remarkably reduces T_c, reflecting novel effects of disorder on both oxypnictide and cuprate superconductors.

4 Conclusions

In summary, detailed lattice parameters, infrared-active optical response, transport and magnetic properties, and electron spin resonance studies have been performed on the pure and oxygen-doped $\mathrm{CaFe_{1-x}Co_xAsF}$ system. It is found that the oxygen doping does not lead to the charge transfer from the CaF(O) charge reservoir layers into the FeAs conduction layers, due to the slight increase of c-axis lattice parameter. In the $\mathrm{CaFe_{0.88}Co_{0.12}AsF}$ superconductor, the substitution of F by O leads to a rapid suppression of superconductivity. We consider besides the charge carrier density, out-of-plane disorder induced by doping in the Ca–F layer plays an important role in the superconductivity.

Acknowledgements This work was supported by the Hundred Talents Program of the Chinese Academy of Sciences and the State Key Project of Fundamental Research of China through Grant 2010CB923403.

References

1. Kamihara, Y., Watanabe, T., Hirano, M., Hosono, H.: J. Am. Chem. Soc. **130**, 3296 (2008)
2. Takahashi, H., Igawa, K., Arii, K., Kamihara, Y., Hirano, M., Hosono, H.: Nature (London) **453**, 376 (2008)
3. Chen, X.H., Wu, T., Wu, G., Liu, R.H., Chen, H., Fang, D.F.: Nature (London) **453**, 761 (2008)
4. Ren, Z.A., Che, G.C., Dong, X.L., Yang, J., Lu, W., Yi, W., Shen, X.L., Li, Z.C., Sun, L.L., Zhou, F., Zhao, Z.X.: Europhys. Lett. **83**, 17002 (2008)
5. Dong, J., Zhang, H.J., Xu, G., Li, Z., Li, G., Hu, W.Z., Wu, D., Chen, G.F., Dai, X., Luo, J.L., Fang, Z., Wang, N.L.: Europhys. Lett. **83**, 27006 (2008)
6. Matsuishi, S., Inoue, Y., Nomura, T., Yanagi, H., Hirano, M., Hosono, H.: J. Am. Chem. Soc. **130**, 14428 (2008)
7. Zhao, J., Huang, Q., de la Cruz, C., Li, S., Lynn, J.W., Chen, Y., Green, M.A., Chen, G.F., Li, G., Li, Z., Luo, J.L., Wang, N.L., Dai, P.C.: Nat. Mater. **7**, 953 (2008)
8. Chen, G.F., Li, Z., Wu, D., Li, G., Hu, W.Z., Dong, J., Zheng, P., Luo, J.L., Wang, N.L.: Phys. Rev. Lett. **100**, 247002 (2008)
9. JCPDS—International Centre for Diffraction Data, 40-1100 (1990)
10. Singh, D.J., Du, M.-H.: Phys. Rev. Lett. **100**, 237003 (2008)
11. Hu, W.Z., Zhang, Q.M., Wanga, N.L.: Physica C **469**, 545 (2009)
12. Tropeano, M., Fanciulli, C., Ferdeghini, C., Marrè, D., Siri, A.S., Putti, M., Martinelli, A., Ferretti, M., Palenzona, A., Cimberle, M.R., Mirri, C., Lupi, S., Sopracase, R., Calvani, P., Perucchi, A.: Supercond. Sci. Technol. **22**, 034004 (2009)
13. Zhao, S.C., Hou, D., Wu, Y., Xia, T.L., Zhang, A.M., Chen, G.F., Luo, J.L., Wang, N.L., Wei, J.H., Lu, Z.Y., Zhang, Q.M.: arXiv:0806.0885
14. Zhang, L., Fujita, T., Chen, F., Feng, D.L., Maekawa, S., Chen, M.W.: arXiv:0809.1474
15. Nomura, T., Inoue, Y., Matsuishi, S., Hirano, M., Kim, J.E., Kato, K., Takata, M., Hosono, H.: J. Cryst. Growth **311**, 358 (2009)
16. Xiao, Y., Su, Y., Mittal, R., Chatterji, T., Hansen, T., Kumar, C.M.N., Matsuishi, S., Hosono, H., Bruechel, Th.: Phys. Rev. B **79**, 060504 (2009)
17. Takeshita, S., Kadono, R., Hiraishi, M., Miyazaki, M., Koda, A., Matsuishi, S., Hosono, H.: Phys. Rev. Lett. **103**, 027002 (2009)
18. Nomura, T., Inoue, Y., Matsuishi, S., Hirano, M., Kim, J.E., Kato, K., Takata, M., Hosono, H.: Supercond. Sci. Technol. **22**, 055016 (2009)
19. Nomura, T., Kim, S.W., Kamihara, Y., Hirano, M., Sushko, P.V., Kato, K., Takata, M., Shluger, A.L., Hosono, H.: Supercond. Sci. Technol. **21**, 125028 (2008)
20. Margadonna, S., Takabayashi, Y., McDonald, M.T., Brunelli, M., Wu, G., Liu, R.H., Chen, X.H., Prassides, K.: Phys. Rev. B **79**, 014503 (2009)
21. Prakash, J., Singh, S.J., Patnaik, S., Ganguli, A.K.: Solid State Commun. **149**, 181 (2009)
22. Li, L.J., Wang, Q.B., Luo, Y.K., Chen, H., Tao, Q., Li, Y.K., Lin, X., He, M., Zhu, Z.W., Cao, G.H., Xu, Z.A.: arXiv:0809.2009
23. Abrikosov, A.A., Gorkov, L.P.: Sov. Phys. JETP **12**, 1243 (1961)
24. Takenaka, K., Watanabe, R., Yamada, H., Tabuchi, M., Takeda, Y., Ikuta, H.: J. Phys. Soc. Jpn. **78**, 073701 (2009)
25. Fujita, K., Noda, T., Kojima, K.M., Eisaki, H., Uchida, S.: Phys. Rev. Lett. **95**, 097006 (2005)